过程与工艺

DOI: 10.12034/j.issn.1009-606X.217390

Determination of sulfhydryl content in CTS–GSH through near-infrared reflectance spectroscopy

Peng ZHANG[1*], Yulu Wang[1], Guocheng ZHU[1], Zhaojie JIAO[2], Wei ZHANG[1]

1. School of Civil Engineering, Hunan University of Science and Technology, Xiangtan, Hunan 411201, China
2. Engineering Research Center for Waste Oil Recovery Technology and Equipment of Ministry of Education,Chongqing Technology and Business University, Chongqing 400067, China

Abstract: The thiolated chitosan (CTS–GSH) was synthesized via the amidation reaction of chitosan (CTS) with reduced glutathione (GSH). A total of 56 samples were scanned with near-infrared reflectance spectroscopy (NIRS) instrument. The characteristic absorption peaks of each band were selected as independent variables, and sulfhydryl content as the dependent variable, the partial least squares (PLS) model was established. Sulfhydryl content was predicted by the PLS, and predicted values were compared with measured values. The results showed that the correlation coefficient of the measured and predicated values of sulfhydryl content was more than 0.9, presenting a good forecasting performance of the model. The difference between the predicted and measured values was nonsignificant, suggesting the feasibility of predicting sulfhydryl content in CTS–GSH through NIRS.

Key words: chitosan–sulfated glutathione; sulfhydryl; near-infrared reflectance spectroscopy; partial least squares; coagulation

CLC No.: X703.1 **Document Code:** A **Article ID:** 1009–606X(2018)04–0757–07

近红外光谱法测定CTS–GSH中巯基含量

张 鹏[1*]， 王雨露[1]， 朱国成[1]， 焦昭杰[2]， 张 伟[1]

1. 湖南科技大学土木工程学院，湖南 湘潭 411201
2. 重庆工商大学废油资源化技术与装备教育部工程研究中心，重庆 400067

摘 要：选取 56 份自制的壳聚糖与谷胱甘肽通过酰胺化反应合成的巯基化壳聚糖(CTS–GSH)样品，对其进行近红外光谱扫描，选取各波段的特征吸收峰作为自变量，以巯基含量为因变量，建立偏最小二乘(PLS)模型预测巯基含量，并将预测值与实测值作比较. 结果表明，预测值与计算值的相关系数大于 0.9，表明模型具有良好的预测性能. 预测值和实测值的差异不显著，表明近红外光谱预测 CTS-GSH 中的巯基含量具有可行性.

关键词：巯基化壳聚糖； 巯基； 近红外光谱； 偏最小二乘法； 混凝

1 INTRODUCTION

Owing to the increased number of mining activities, including dressing and smelting of metal mines, a large number of metal ions are inevitably released into water bodies[1–3]. These metal ions seriously damage water environments[4,5]. Current methods for the treatment of wastewater contaminated with heavy metals are often divided into two categories: physical and chemical methods and biological methods (biochemistry). Traditional physical and chemical methods mainly include

Received: 2017–11–16, **Revised:** 2018–01–18, **Published online:** 2018–06–07
Foundation item: Supported by National Natural Science Foundation of China (No. 41502331, 51408215); Hunan Natural Science Foundation (No. 2018JJ3174)
Biography: ZHANG Peng (1982–), male, Datong City, Shanxi Province, doctor, associate professor, engaged in flocculation/coagulation Science and technology, E-mail: zhangpeng388@126.com.

引用格式： Zhang P, Wang Y L, Zhu G C, et al. Determination of sulfhydryl content in CTS–GSH through near-infrared reflectance spectroscopy. Chin. J. Process Eng., 2018, 18(4): 757–763, DOI: 10.12034/j.issn.1009-606X.217390.

adsorption[6–8], chemical reduction precipitation, photocatalysis[9], membrane separation[10–12], ion exchange[13–15], coagulation/flocculation[16–18] and electrochemical method[19,20]. Biological methods include microbial remediation and phytoremediation[21–23]. The coagulation method has been widely used in the pretreatment of aquatic heavy metals owing to its low cost and simple operation, which is one of the most effective methods in traditional physical and chemical methods[24–26]. In accordance with the theories of coordination chemistry and hard and soft acids and bases, molecules containing sulfate (S) and heavy metal ions should have strong coordination capability. In theory, the introduction of S into a coagulant facilitates the removal of heavy metals from wastewater. Reduced glutathione (GSH) contains various coordinating groups, such as sulfhydryl, amide, carboxyl and amino groups[27]. GSH is a suitable monomer for the synthesis of coagulants that effectively remove heavy metals. CTS–GSH is a polymeric coagulant obtained via the amidation reaction between chitosan (CTS) and GSH. High-content sulfhydryl groups in coagulants effectively removes heavy metals because of the excellent coordination capability between the sulfhydryl groups and heavy metal ions[27]. The differences between the theoretical and actual contents of sulfhydryl groups in an actual product are attributed to the incomplete conversion of GSH monomers during CTS–GSH production by the polymerization reaction between CTS and GSH. Sulfhydryl content is an important indicator of the performance of CTS–GSH. Therefore, effective evaluation of the sulfhydryl content in CTS–GSH is extremely important.

UV (ultraviolet) spectrophotometry[28], high-performance liquid chromatography and electrochemical method are frequently employed for the quantification of sulfhydryl content. These methods are complex with respect to preprocessing, time consuming, and expensive and require the destruction of samples, therefore, the rapid quantification of actual samples and preventing their damage is difficult. Near-infrared spectroscopy (NIRS) is effective in obtaining the chemical information of organic groups[29]. At present, NIRS is widely applied in agriculture[30–32], medicine[33], and environmental research for the characterization of the composition of organic samples[34]. In addition, preprocessing of samples is optional in NIRS spectral scanning. Thus, NIRS is a convenient, low-cost, and rapid method. In the present study, we adopted UV spectrophotometry and NIRS to analyze sulfhydryl content in CTS–GSH. Results showed that sulfhydryl content in CTS–GSH can be rapidly and accurately quantified through NIRS.

2 MATERIAL AND METHODS

2.1 Materials Preparation

The CTS–GSH was prepared through amidation reaction by using CTS and GSH as the main raw material, N-Hydroxy succinimide (NHS) as protective agent, 1-Ethyl-3-(3-dimethyllaminopropyl)carbodiie hydrochlide (EDC) as cross-linking agent. And the steps for CTS–GSH preparation were as follows: Firstly, a given volume of CTS was swelling with 1.0 mol/L HCl solution in a 100 mL beaker, then added a certain volume of pure water for fully dissolved and transferred into a 250 mL triangle flask. Secondly, added a certain quality of EDC, NHS, GSH into the 250 mL triangle flask, adjust the solution pH value, keep on reacting for several hours under magnetic stirring, and then got a certain viscosity of transparent liquid, which was the crude product. Thereafter, thecrude product and ethanol volume ratio controlled for 1:5 and oscillated uniform for 1 h, then centrifugated at 3000 r/min for 10 min, the pure product was obtained by using ethanol washed solid material which was the supernatant after filtration.

A total of 56 CTS–GSH samples were collected for analysis. All the samples were pulverized with mortar and pestle and then sieved through 32 meshes (500 μm).

2.2 Spectrographic Determination of Sulfhydryl Content in CTS–GSH

A small amount of the liquid product of CTS–GSH and 4,4'-dithiodipyridine acetonitrile solution were prepared and placed into a volumetric

flask. The sample was then diluted with NaH_2PO_4–EDTA buffer solution and then mixed evenly until a reaction was induced. Finally, absorbance was measured at 324 nm with a TU-1910 UV–Vis spectrophotometer (Beijing Purkinje General Instrument Co., Ltd., China). Sulfhydryl content in each sample was calculated in accordance with the standard curve. Each sample was duplicated three times, and the mean values were used.

2.3 Analysis Instrument

NIRS data was collected with a NIRQuest-512 near-infrared spectrometer (American Ocean Optics corporation). The optical resolution was 4 nm, and NIRS was furnished with spectra suite spectroscopy platform software under the wavelength range of 900.00~1 700.00 nm. The spectra were sampled eight times on average at 48 ms each time, and the smoothness was 3. The spectrometer was preheated for 30 min for the reduction of dark current prior to sampling.

2.4 Partial Least Squares (PLS) Regression

PLS is capable of analyzing the mixture information of overlapping map without a single pure component information. This method is more effective than multiple and principal component regressions. The principle of PLS is that the observed data is divided into several regions according to their sources, and each region may be described by a set of feature vectors, which is a linear function of the initial observation variables. In the same area, they are mutually orthogonal. In this study, PLS was established between p dependent variables $y_1, y_2, \cdots, y_p$ and m independent variables $x_1, x_2, \cdots, x_m$. For convenience, the p dependent variables and m independent variables were assumed standard, and the N times of the standard observation data matrix of these variables were recorded in accordance with the procedure specified in the succeeding paragraph.

$$F_0=\begin{pmatrix} y_{11} & \mathrm{K} & y_{1p} \\ \mathrm{M} & \mathrm{O} & \mathrm{M} \\ y_{n1} & \mathrm{L} & y_{np} \end{pmatrix}, \qquad E_0=\begin{pmatrix} x_{11} & \mathrm{K} & x_{1m} \\ \mathrm{M} & & \mathrm{M} \\ x_{n1} & \mathrm{L} & x_{nm} \end{pmatrix}. \tag{1}$$

PLS regression shows major modeling composition and the features of related typical and linear regressive analyses. PLS provides a reasonable regressive model and derives research findings similar to those obtained using main composition and related typical analyses. Furthermore, this approach offer better and deeper information than other techniques.

2.5 Preprocessing of Near-infrared Spectrum Data

Data analysis usually requires data normalization (also statistical data indexation), which mainly includes data convergence and nondimensionalization. Data convergence is mainly used for problems due to the differences among data types. Direct aggregation of different types of indices cannot accurately reflect the consolidated results of different forces. Thus, the nature of the inverted index data must be changed such that the actions of all indices on the test program converge before aggregation and correct results are obtained. Data nondimensionalization is mainly designed for data comparability.

Spectrum data are standardized to zoom on them in accordance with a certain ratio and fall into a small specific area. This method is data normalization based on the mean and standard deviation of raw data. In this process, the unit limitation of the data is removed and transferred into a nondimensional pure data for the comparison and weighing different units or dimension indicators. The most commonly used data normalization method is deviation normalization, which is based on statistical theories. This method is also called standard deviation normalization.

In this study, Z-score standard processing was adopted in which data meet the standard normal distribution requirements with a standard gap of 1 and an average mean of 0. The transfer formula is depicted as follows:

$$x^*=(x-u)/\sigma, \tag{2}$$

where, x is the sample date, u is the average value of the sample date, and σ is the standard deviation of the sample date.

2.6 Near-infrared Technology

Near-infrared technology, which is a modern spectroscopic technique, involves modern electronic technology, spectroscopy, computer technology, and stoichiometry. Its inspection process mainly includes a

representative sample and an unknown sample. In a representative sample, optical data are tested with a standard method, spectral data and data detected by the standard method are associated mathematically, and the spectral data after conversion and data detected by the standard method are calculated by regression. Therefore, a calibration equation is obtained, and a data model is established. By contrast, an unknown sample requires scanning before analysis, so the component content of the test sample must be calculated on the basis of spectra and model. Compared with conventional analytical techniques, NIRS can determine several or dozens of types of data of a sample simultaneously within tens of seconds or less through simple measurements.

3 RESULTS AND DISCUSSION

3.1 Determination of Sulfhydryl Content

The sulfhydryl content of CTS–GSH was measured at an adsorption wavelength (λ) of 412 nm through UV spectrophotometry. UV spectrophotometry and near-infrared spectroscopy was compared with respect to their accuracies in determining sulfhydryl content in CTS–GSH. The results were shows in Table 1. It can be seen that CTS–GSH sulfhydryl group content in 56 shares of coagulants was analyzed through UV spectrophotometry. The distribution scope of the result varied between 3.03% and 6.97%, with a mean value of 5.94% and a standard deviation of 0.76%. The distribution scope of the predicted NIRS results ranged from 3.14% to 6.94%, with a mean value of 5.93% and a standard deviation of 0.72%. It could be seen that NIRS with the smaller standard deviation than UV spectrophotometry. The smaller the standard deviation, the better the precision. The accuracy in determining sulfhydryl content in CTS–GSH result also showed that NIRS and UV spectrophotometry had no considerable differences, indicating that NIRS had a high degree of reliability.

Table 1 Sulfhydryl content determined by UV spectrophotometry

Parameter	UV spectrophotometry/%	NIRS/%
Mean	5.94	5.93
Maximum value	6.97	6.94
Minimum value	3.03	3.14
Standard deviation	0.76	0.72

3.2 Sample Near-infrared Reflection Spectrum and PLS Model Structure

A total of 56 CTS–GSH samples were scanned through NIRS. The results were presented in Fig.1. It can be seen that CTS–GSH contained functional groups, such as sulfhydryl, amide, carboxyl and amino groups and displayed an obvious absorption peak within a wavelength of 899.22~1 721.76 nm. The same sample indicated different absorption peaks, whereas various samples exhibited evident peak differences in the same wavelength absorption peak. This condition reflected the applicability of CTS–GSH near-infrared absorption spectrum to quantitatively analyze sulfhydryl group contents.

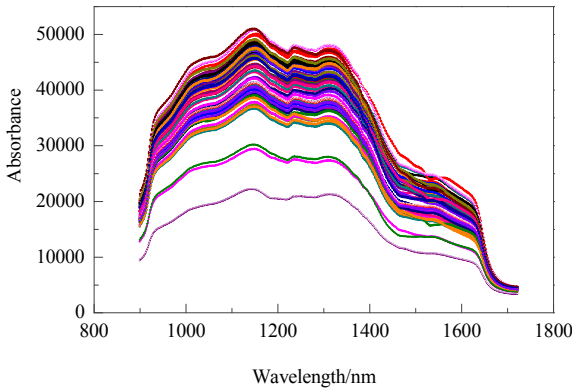

Fig.1 NIR spectra of CTS–GSH

The near-infrared absorption spectrum data of CTS–GSH were used as bases for the establishment of the quantitative analysis model of the CTS–GSH sulfhydryl group content. A standard method was adopted for data processing, which includes the pretreatment of data. The absorption values of five peaks were used as independent variables (1 068.83, 1 221.71, 1 283.05, 1 465.59 and 1 677.72 nm), whereas monomer content was used as the dependent variable for the establishment of the PLS model.

3.3 PLS Model Validation

The developed calibration PLS formula was as follows:

$$Y = 3.12\times10^{-5}X_1 + 6.92\times10^{-5}X_2 + 5.52\times10^{-5}X_3 - 1.58\times10^{-5}X_4 - 2.61\times10^{-5}X_5 + 0.2623, \quad (3)$$

where, Y is the CTS–GSH sulfhydryl group content, X is the spectral absorbance, and X_1, X_2, X_3, X_4, and X_5

are the absorbance values corresponding to absorbance wavelengths of 1068.83, 1221.71, 1283.05, 1465.59 and 1677.72 nm, respectively.

Furthermore, 19 CTS–GSH samples with different sulfhydryl group contents were adopted for prediction. The predicted values were showed in Table 2, and the prediction distribution was indicated in Fig.2. As shown in Table 2, the predicted value of the CTS–GSH was proximate to the measured value. The average content of 19 sulfhydryl group was 5.90%, whereas the average predicted value of sulfhydryl group contents was 5.85%. To inspect the reliability of the prediction method on the CTS–GSH sulfhydryl group content using the near-infrared model, *t* inspection was adopted to verify the new method. A certain CTS–GSH sample was selected randomly for inspection. Then, UV spectrophotometry was adopted to test the sample with 6.42% sulfhydryl group content, and near-infrared spectrum prediction method was used for the prediction of the selected sample for six times. The results were demonstrated in Table 3 in detail.

Table 2　Comparison between measured and predicted value of sulfhydryl content

Sample	1	2	3	4	5	6	7	8	9	10
Measured value/%	6.11	6.56	6.53	6.11	5.56	6.63	5.65	6.29	5.94	5.77
Predicted value/%	6.10	6.50	6.45	6.08	5.56	6.55	5.65	6.22	5.94	5.76
Sample	11	12	13	14	15	16	17	18	19	
Measured value/%	6.73	5.37	6.98	6.07	5.36	6.27	5.29	3.03	5.44	
Predicted value/%	6.65	5.38	6.92	6.01	5.33	6.25	5.26	3.14	5.44	

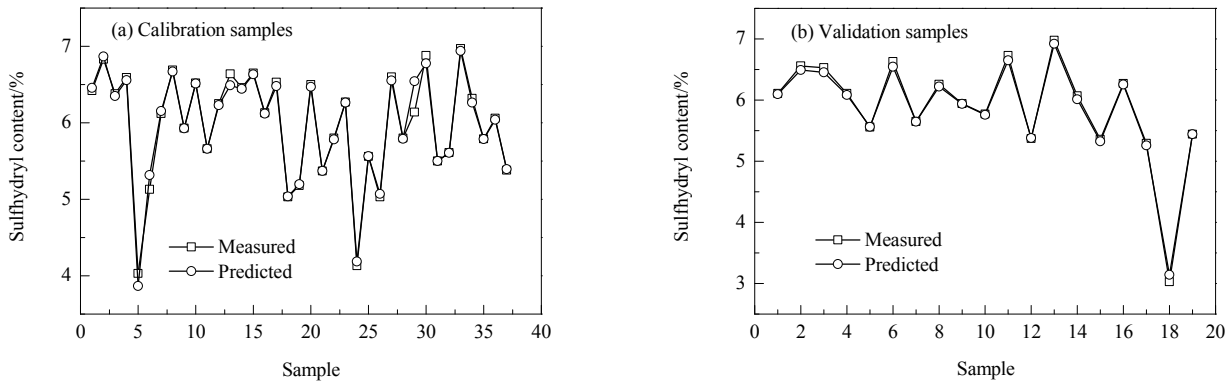

Fig.2　Trends of measured sulfhydryl content and predicted value

Table 3　Predicted value of sulfhydryl content

Number of measurement	1	2	3	4	5	6
Predicted value/%	6.41	6.50	6.45	6.48	6.40	6.39

4D inspection was carried out on the prediction result of a single sample. The result displayed the prediction value within the normal scope, indicating that it was effective. *t* inspection was performed to obtain six prediction results for a single sample and determined the *t* distribution form. With obvious levelα=0.05, and freedom of f =5, $t_{0.05,5}$ was equal to 2.571 and t=1.088<$t_{0.05,5}$. The inspection result showed that the surveyed results obtained through UV spectrophotometry and near-infrared prediction had no considerable differences, indicating that the near-infrared prediction method had a high degree of reliability.

t inspection was performed on the prediction values of 19 shares of different samples, and *t* distribution form was identified. With obvious level α=0.05 and freedom of f =18, $t_{0.05,18}$ is equal to 2.101 and t=0.149<$t_{0.05,18}$. The inspection result indicated that the difference between the characteristic peak absorption value, as the independent variable to establish a PLS model, and that measured by sedimentation and titration was nonsignificant. Therefore, the model is feasible.

3.4　Correlation Analyses of the Determination Effect of Sulfhydryl Content of CTS–GSH

Near-infrared spectrum method was adopted to inspect the sulfhydryl group content of the sample, the correlation coefficient (R^2) of the simulated and

surveyed values of external verification was above 0.90, implying that the prediction model was favorable. Two-thirds of the sample was sieved for modeling (calibration sample), and one-third of the sample was adopted for the model test (validation sample). From Fig.3, it can be seen that the relationship between the surveyed and NIRS predicted values obtained through UV spectrophotometry (the horizontal coordinate refers to the surveyed value of UV spectrophotometry, whereas the vertical coordinate represents the NIRS predicted value). In both results, the R^2 values were higher than 0.90, suggesting a favorable linear relationship between the predicted and measured values of the sulfhydryl group content and a favorable prediction effect. Therefore, NIRS can be used for the accurate and rapid prediction of sulfhydryl group content in CTS–GSH. The scatter diagram (Fig.2) and the prediction trend (Fig.3) between the measured sulfhydryl group contents and the predicted value demonstrated a favorable relationship, and the sulfhydryl group content predicted by NIRS was highly accurate.

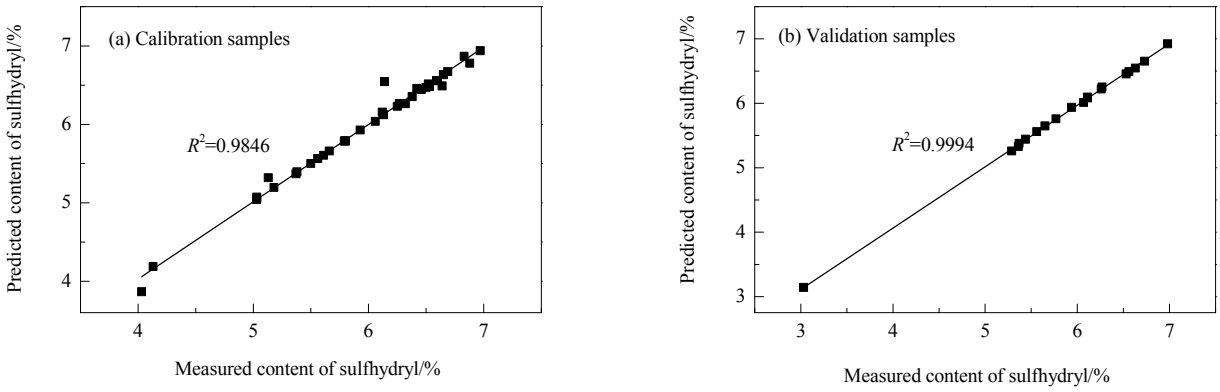

Fig.3 Correlation of measured content of sulfhydryl with predicted value

4 CONCLUSION

NIRS was used for the prediction of sulfhydryl group content in the fabricated the thiolated chitosan (CTS–GSH) sample. PLS arithmetical conversion was used for the establishment of the NIRS calibration model capable of predicting sulfhydryl group content in CTS–GSH. The comparison between the predicted and measured values by UV spectrophotometry presents two main findings:

(1) The correlation coefficient of external verification was larger than 0.90.

(2) *t* inspection results reflected no significant difference between the predicted and observed sulfhydryl group contents. The error caused by the artificial factors in traditional tests can be removed through NIRS, and the test effect of Near-infrared spectroscopy (NIRS) may be superior to that of the UV spectrophotometry. NIRS is capable of rapidly and accurately predicting sulfhydryl group content in CTS–GSH.

REFERENCE

[1] Brocca L, Morbidelli R, Melone F, et al. Soil moisture spatial variability in experimental areas of central Italy [J]. J. Hydrol., 2007, 333(2/4): 356–373.

[2] Itskos G, Koutsianos A, Koukouzas N, et al. Zeolite development from fly ash and utilization in lignite mine-water treatment [J]. Int. J. Miner. Process., 2015, 139: 43–50.

[3] Kumar A, Maiti S K. Assessment of potentially toxic heavy metal contamination in agricultural fields, sediment, and water from an abandoned chromite-asbestos mine waste of Roro hill, Chaibasa, India [J]. Environ. Earth Sci., 2015, 74(3): 1–17.

[4] Wingenfelder U, Hansen C, Furrer G, et al. Removal of heavy metals from mine waters by natural zeolites [J]. Environ. Sci. Technol., 2005, 39(12): 4606–4613.

[5] Abongwa P T, Geyer C, Puckette J. Investigating the effectiveness of mineral precipitate as a tool in the removal of heavy metals from mine waters [C]//AGU Fall Meeting. AGU Fall Meeting Abstracts, 2014, 93(8): 18–23.

[6] Sounthararajah D P, Loganathan P, Kandasamy J, et al. Effects of humic acid and suspended solids on the removal of heavy metals from water by adsorption onto granular activated carbon [J]. Int. J. Environ. Res. Public. Health, 2015, 12(9): 10475–10489.

[7] Matouq M, Jildeh N, Qtaishat M, et al. The adsorption kinetics and modeling for heavy metals removal from wastewater by moringa, pods [J]. J. Environ. Chem. Eng., 2015, 3(2): 775–784.

[8] Matłok M, Petrus R, Warchoł J K. Equilibrium study of heavy metals adsorption on Kaolin [J]. Ind. Eng. Chem. Res, 2015,

54(27): 6975–6984.

[9] Sreekantan S, Lai C W, Zaki S M. The influence of lead concentration on photocatalytic reduction of Pb(II) ions assisted by Cu–TiO_2 nanotubes [J]. Int. J. Photoenergy, 2014, 2014: 1–7.

[10] Mavrov V, Erwe T, Blöcher C, et al. Study of new integrated processes combining adsorption, membrane separation and flotation for heavy metal removal from wastewater [J]. Desalination, 2003, 157(1): 97–104.

[11] Muthukrishnan M, Guha B K. Heavy metal separation by using surface modified nanofiltration membrane [J]. Desalination, 2006, 200(1): 351–353.

[12] Ge Y Y, Yuan Y, Wang K T, et al. Preparation of geopolymer-based inorganic membrane for removing Ni(2+) from wastewater [J]. J. Hazard. Mater., 2015, 299: 711–718.

[13] Feng D, Aldrich C, Tan H. Treatment of acid mine water by use of heavy metal precipitation and ion exchange [J]. Miner. Eng., 2000, 13(6): 623–642.

[14] Kim S J, Lim K H, Joo K H, et al. Removal of heavy metal-cyanide complexes by ion exchange [J]. Korean J. Chem. Eng., 2002, 19(6): 1078–1084.

[15] Plazinski W, Rudzinski W. Modeling the effect of surface heterogeneity in equilibrium of heavy metal ion biosorption by using the ion exchange model [J]. Environ. Sci. Technol., 2009, 43(19): 7465–7471.

[16] Liu Y L, Cao C C, Ning S T, et al. Research on the effects of coagulation process on the removal of humic acid and heavy metal [J]. Industrial Safety & Environmental Protection, 2015, 61(1/2): 171–180 (in Chinese).

[17] Oladoja N A. Headway on natural polymeric coagulants in water and wastewater treatment operations [J]. J. Water Process Eng., 2015, 6: 174–192.

[18] Shamsnejati S, Chaibakhsh N, Pendashteh A R, et al. Mucilaginous seed of ocimum basilicum, as a natural coagulant for textile wastewater treatment [J]. Ind. Crops Prod., 2015, 69: 40–47.

[19] Mouedhen G, Feki M, De P M, et al. Electrochemical removal of Cr(VI) from aqueous media using iron and aluminum as electrode materials: towards a better understanding of the involved phenomena [J]. J. Hazard. Mater., 2009, 168(2/3): 983–991.

[20] Barrera-Díaz C, Lugo-Lugo V, Roa-Morales G, et al. Enhancing the electrochemical Cr(VI) reduction in aqueous solution [J]. J. Hazard. Mater., 2011, 185(2/3): 1362–1368.

[21] Cheng Y J, Yan F B, Feng H, et al. Bioremediation of Cr(VI) and immobilization as Cr(III) by ochrobactrum anthropi [J]. Environ. Sci. Technol., 2010, 44(16): 6357–6363.

[22] Kramer D M, Puzon G J, Xun L, et al. Formation of soluble organo–chromium(III) complexes after chromate reduction in the presence of cellular organics [J]. Environ. Sci. Technol., 2005, 39(8): 2811–2817.

[23] Kumari M, Tripathi B D. Efficiency of phragmites australis, and typha latifolia, for heavy metal removal from wastewater [J]. Ecotoxicolo. Environ. Saf., 2015, 112: 80–86.

[24] Zhang P, Ren B. Inverse emulsion polymerization of dimethyl diallyl ammonium chloride and acrylamide for water treatment [J]. Asian J. Chem., 2013, 25(7): 3966–3970.

[25] Zhu G C, Zheng H L, Chen W, et al. Preparation of a composite coagulant: polymeric aluminum ferric sulfate (pafs) for wastewater treatment [J]. Desalination, 2012, 285(1): 315–323.

[26] Golbaz S, Jafari A J, Rafiee M, et al. Separate and simultaneous removal of phenol, chromium, and cyanide from aqueous solution by coagulationprecipitation: mechanisms and theory [J]. Chemical Engineering Journal, 2014, 253(7): 251–257.

[27] Liu X R, Hong W W, Deng Y H. Determination of thiol content in thiolated chitosan by 4,4′ -dithiodipyridine [J]. Journal of Shenyang Pharmaceutical University, 2013, 30(2): 120–125 (in Chinese).

[28] Dai C Y, Gao X Y, Tang B, et al. Determination of the contents of chlorogenic acid and phillyrin of shuanghuanglian oral fluid using NIRS [J]. Spectrosc. Spect. Anal., 2010, 30(2): 358–362 (in Chinese).

[29] Wang J J, Cui L J, Gao W X, et al. Prediction of low heavy metal concentrations in agricultural soils using visible and near-infrared reflectance spectroscopy [J]. Geoderma, 2014, 216(4): 1–9.

[30] Song H Y, Qin G. Study on the calibration transfer of near infrared spectroscopy model for soil organic matter content prediction by using FIR [J]. Spectrosc. Spect. Anal., 2015, 35(12): 3360–3363 (in Chinese).

[31] Todorova M, Mouazen A M, Lange H, et al. Potential of near-infrared spectroscopy for measurement of heavy metals in soil as affected by calibration set size [J]. Water Air Soil Poll., 2014, 225(8): 2036–2055.

[32] Okparanma R N, Coulon F, Mayr T, et al. Mapping polycyclic aromatic hydrocarbon and total toxicity equivalent soil concentrations by visible and near-infrared spectroscopy [J]. Environ. Pollut., 2014, 192: 162–170.

[33] Li C Y, Zhang G Y, Dong X Y, et al. Antioxidant property prediction of methanol extracts of crude drug based on near infrared spectroscopy [J]. Spectrosc. Spect. Anal., 2017; 37(8): 2402–2405 (in Chinese).

[34] Zheng H L, Zhang P, Chen Y Z, et al. Determination of cationic degree in PDA with near infrared reflectance spectroscopy [J]. Spectrosc. Spect. Anal., 2012, 32(2): 334–338 (in Chinese).